24. T. A. Jones, *J. Appl. Crystallogr.* 11, 272 (1978).
25. SHELX-93; G. Sheldrick, University of Göttingen.
26. Z. Otwinowski, in *Proceedings of the CCP4 Study Weekend*, L. Sawyer, N. Issacs, S. Bailey, Eds. (Science and Engineering Research Council, Daresbury Laboratory, 1993), pp. 56–62.
27. A number of parallel-stranded guanine tetraplex models were generated on the basis of the conformational details determined in solution by NMR (*12*). These were then incrementally over- and underwound to generate a series of model structures for molecular replacement with AMORE (*19*). The optimal model yielded a set of highest peaks related by noncrystallographic fourfold symmetry. Translation function solutions were found that were consistent with the noncrystallographic symmetry suggested by the Patterson function (*20*). These were initially refined by simulated annealing with X-PLOR (version 3.1) (*21*), and only restraints to ensure base planarity were used. An automated refinement procedure followed (ARP) (*22*) that reiteratively adjusts the water structure of the model. The resulting map was sufficiently clear to reveal that the derived solution was false, in that one of the tetraplexes in each stacked pair was spatially out of register by one base step along the helical axis. The error was manually rectified, and the genuine solution rapidly refined with X-PLOR and ARP, combined with least squares minimization [PROTIN/PROLSQ (*23*)] with the use of a modified stereochemical dictionary to an *R* factor of 18.8%. Extensive rebuilding was undertaken throughout with the use of FRODO (*24*), resulting in the incorporation of 27 of the 32 thymine bases. Further refinement, including anisotropic temperature factors and the introduction of hydrogen atoms, was then undertaken using SHELX-93 (*25*) to a final *R* factor of 12.4% for the data from 8.0 to 1.2 Å. The free *R* factor (*21*) was 17.6% for 1 out of 10 of the reflections being excluded from the refinement procedure. Even after anisotropic refinement, there was no clear density for the five missing thymine bases, presumably because of high thermal disorder, and these were excluded from the final model.
28. We are grateful to J. Navaza for help with AMORE; U. Pieles for mass spectrometry; E. Dodson, A. Lapthorn, F. Aboul-ela, and Z. Otwinowski for helpful suggestions; N. Isaacs for support; and the Cancer Research Campaign and Medical Research Council for financial assistance. The coordinates will be deposited with the Brookhaven Data Bank and can be obtained immediately by contacting B.L. (ben@chem.glasgow.ac.uk).

7 March 1994; accepted 17 May 1994

The Three-Dimensional Crystal Structure of the Catalytic Core of Cellobiohydrolase I from *Trichoderma reesei*

Christina Divne, Jerry Ståhlberg, Tapani Reinikainen, Laura Ruohonen, Göran Pettersson, Jonathan K. C. Knowles, Tuula T. Teeri, T. Alwyn Jones*

Cellulose is the major polysaccharide of plants where it plays a predominantly structural role. A variety of highly specialized microorganisms have evolved to produce enzymes that either synergistically or in complexes can carry out the complete hydrolysis of cellulose. The structure of the major cellobiohydrolase, CBHI, of the potent cellulolytic fungus *Trichoderma reesei* has been determined and refined to 1.8 angstrom resolution. The molecule contains a 40 angstrom long active site tunnel that may account for many of the previously poorly understood macroscopic properties of the enzyme and its interaction with solid cellulose. The active site residues were identified by solving the structure of the enzyme complexed with an oligosaccharide, *o*-iodobenzyl-1-thio-β-cellobioside. The three-dimensional structure is very similar to a family of bacterial β-glucanases with the main-chain topology of the plant legume lectins.

Cellulose is the most abundant renewable resource on Earth, accounting for about half of the organic material in the biosphere. In addition to its ecological and commercial importance, the high degree of crystallinity of the substrate makes cellulose degradation a problem of fundamental interest. Cellulolytic fungi produce exoglucanases or cellobiohydrolases (CBH, 1,4-β-D-glucan cellobiohydrolase, E.C. 3.2.1.91) that hydrolyze crystalline cellulose by cleavage from chain ends (*1*). They act synergistically with endoglucanases (EG, 1,4-β-D-glucanohydrolase, E.C. 3.2.1.4) that primarily hydrolyze the disordered, amorphous regions of cellulose, cutting at internal glycosidic bonds (*1*).

C. Divne, J. Ståhlberg, T. A. Jones, Department of Molecular Biology, Uppsala University, Biomedical Centre, Box 590, S-751 24 Uppsala, Sweden.
T. Reinikainen, L. Ruohonen, T. T. Teeri, VTT Biotechnology and Food Research, Post Office Box 1500, FIN-02044 VTT, Espoo, Finland.
G. Pettersson, Department of Biochemistry, Uppsala University, Biomedical Centre, Box 576, S-751 23 Uppsala, Sweden.
J. K. C. Knowles, Glaxo Institute for Molecular Biology, 14 Chemin des Aulx, 1228 Plan-les-Ouates, Geneva, Switzerland.

*To whom correspondence should be addressed.

The cellobiohydrolase CBHI is probably the key enzyme needed for the efficient hydrolysis of native crystalline cellulose. It is the most abundant cellulase produced by the filamentous fungus *Trichoderma reesei*, and the removal of its gene reduces overall activity on crystalline cellulose by 70% (*2*). It exhibits the strongest synergy with other *T. reesei* and bacterial cellulases (*3*). Because CBHI acts synergistically with the other cellobiohydrolase (CBHII) produced by *T. reesei* (*4*), it has been suggested that one or both of the enzymes may possess endoglucanase activity (*5*). Cellobiohydrolase I has been classified on the basis of its amino acid sequence as a family C enzyme (*6*). This family includes both exo- and endoglucanases which cleave the β(1 → 4) glycosidic bond by a double-displacement mechanism, resulting in retention of configuration of the product, cellobiose (*7*).

Cellobiohydrolase I is a two-domain enzyme, consisting of a large catalytic core linked to a small cellulose-binding domain by a heavily glycosylated linker region (*8*). The structure of the core was solved by the standard method of multiple isomorphous

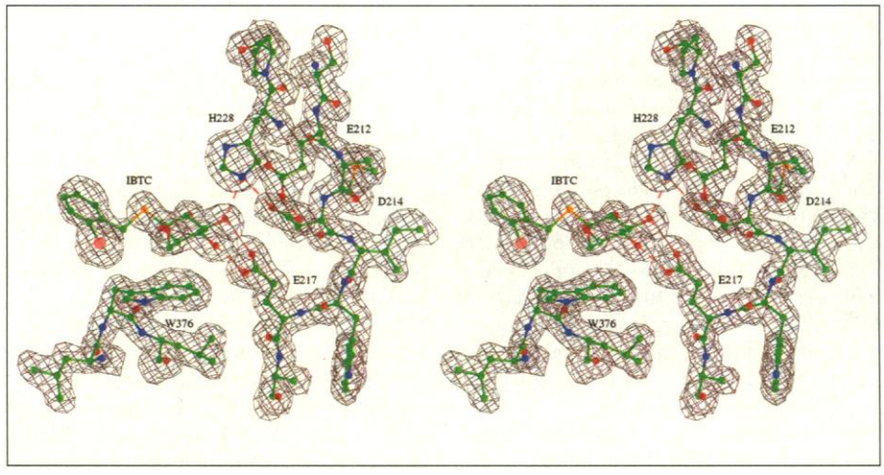

Fig. 1. Electron density of the active site residues. The map was calculated with $2|F_{obs}| - |F_{calc}|$ amplitudes, and phases were calculated from the final model. The ligand, *o*-iodobenzyl-1-thio-β-D-glucose, is labeled IBTC and hydrogen bonds are indicated by dashed lines.

replacement (MIR), and a model was refined to a crystallographic R factor of 18.1% at 1.8 Å resolution (Table 1 and Fig. 1). It consists of a large, single domain with overall dimensions of approximately 60 Å by 50 Å by 40 Å (Fig. 2). About one-third of this 434-residue domain is arranged in two large antiparallel β sheets that stack face-to-face to form a β sandwich. Except for four short α helices, the rest of the protein consists almost entirely of loops connecting the β strands. These loops are partly stabilized by nine of the ten disulfide bridges present in the structure. The two β sheets are highly curved, forming concave and convex faces that contain seven and eight antiparallel β strands, respectively. The interface between the sheets comprises a considerable volume which is packed mostly with hydrophobic side chains but contains one hydrophilic patch formed by residues of both sheets (Glu^{223} from the concave face and Thr^{292}, Arg^{302}, Tyr^{304}, and Gln^{313} from the convex face). Most of the loops between strands in the convex sheet are short, whereas those in the concave sheet and the connections between sheets are longer. Together with local twists in some of the strands, this creates a ~40 Å long tunnel that runs the length of the concave sheet (Fig. 3). The tunnel is the binding site of the cellobioside derivative and the probable active site (*9*).

Table 1. MIR data and crystallographic methods. The crystals belong to space group $P2_12_12$, and the cell dimensions are a = 84.0 Å, b = 86.2 Å, and c = 111.8 Å. The structure was solved by standard MIR methods, making extensive use of density modification and averaging, and has been refined with reciprocal space methods with tight stereochemical restraints (*29*). The second heavy atom derivative was made with a mutant enzyme where a free cysteine was introduced at Ser^{128} by site-directed mutagenesis.

Property	Compound		
	Native	Pb $(CH_3COO)_2$	S128C/ merthiolate
Resolution (Å)	1.81	1.99	1.81
Measurements	99089	131433	92263
Unique reflections	65174	45728	39965
Data to 2.0 Å (%)	95.5	81.4	62.2
Data in highest	52.0	29.0	25.5
Resolution bin (%)	(1.87 to 1.81 Å)	(2.06 to 1.99 Å)	(1.87 to 1.81 Å)
R_{merge}*	4.3	8.3	9.0
R_{deriv}†	(15 to 2.5 Å)	18.7	17.7
R_{Cullis}‡		0.63	0.63
Phasing power§		1.8	1.4
Number of sites		6	2

*$R_{merge} = [\Sigma|I - < I >|/\Sigma< I >] \times 100$. †$R_{deriv} = \Sigma||F_{PH}| - |F_P||/\Sigma F_{PH}$. ‡$R_{Cullis} = \Sigma||F_{PH(obs)}| - |F_{PH(calc)}||/\Sigma||F_{PH(obs)}| - |F_{P(obs)}||$ for centric reflections. §Phasing power = mean value of the heavy atom vector divided by the lack of closure.

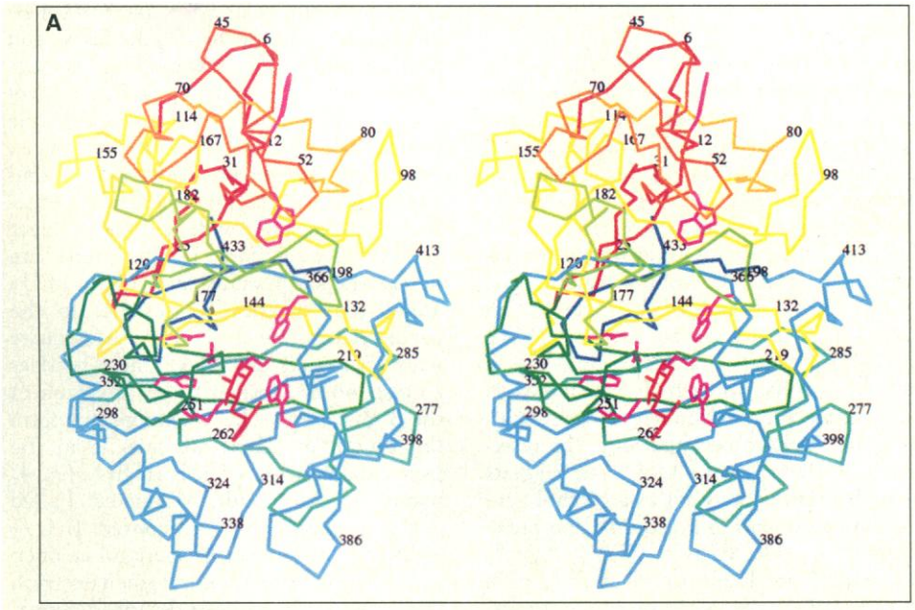

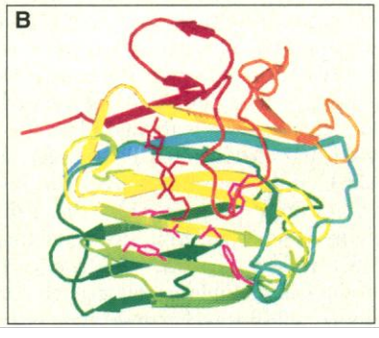

Fig. 2. (**A**) Cα stereo drawing of CBHI with a color ramping scheme where the NH_2-terminal residues appear red and the COOH-terminal residues are blue. The active site residues and ligand are drawn in magenta and red, respectively. The view is approximately orthogonal to the concave top face of the β sandwich. (**B**) For comparison, the β-glucanase is drawn from the same view with color ramping of the secondary structure elements.

The structure of CBHI is very different from the structures of the other four cellulases that have been determined: the catalytic core of CBHII from the fungus *T. reesei* (*10*) and the related endoglucanase E230 from the fungus *Thermomonospora fusca* (*11*), the thermostable bacterial endoglucanase CelD from *Clostridium thermocellum* (*12*), and the fungal endoglucanase EGV from *Humicola insolens* (*13*). Both cellobiohydrolases contain an active site tunnel. Although the tunnel of CBHI is about twice as long as that observed in CBHII, they are both built up from loops extending from a structural motif; in the case of CBHI, several loops extend from the β sandwich core, and in CBHII two long loops extend from the COOH-terminal end of a modified triose isomerase barrel. The sides of both tunnels are formed by side chains involved in a complex network of hydrogen bonds and salt links and are rich in amino acids that are known to interact with sugars (*14*), especially tryptophan residues. There are three tryptophans in CBHII and four in the CBHI tunnel. Both tunnels are flattened to accommodate glucose units, but in CBHI a point at the center forces the cellulose chain to adopt something other than an extended conformation (Fig. 3). In both enzymes, the active site is positioned such that the product, cellobiose, is just enclosed by the tunnel.

We estimate that the CBHI tunnel has seven glucosyl binding sites (A to G), in agreement with other binding studies (*15*). The ligand *o*-iodobenzyl-1-thio-β-D-cellobioside (IBTC) binds to one entrance (Fig. 2) with the aromatic group in site A and a glucosyl unit in B. No interpretable electron density exists for a second glucosyl unit (Fig. 1). Because CBHI can degrade cello-

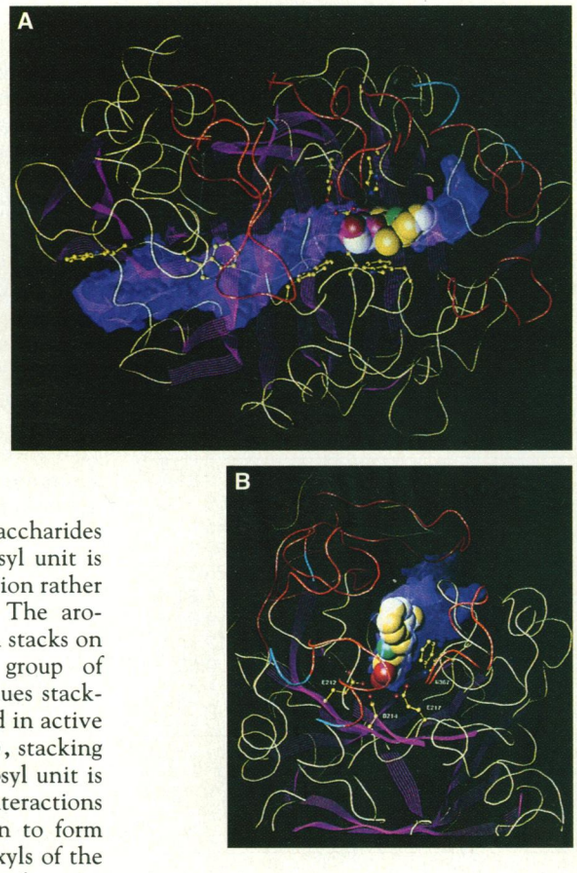

Fig. 3. The active site tunnel of CBHI drawn as a semi-transparent surface. The active site residues and ligand are included. The views are (**A**) orthogonal to the tunnel and (**B**) along the tunnel. The β sandwich is indicated by a magenta ribbon. The Cα trace is colored red to indicate loops that are expected to be deleted in the related endoglucanase EGI of *T. reesei*. Because of low sequence identity, some loops are difficult to delimit precisely. Therefore, these are in blue with red representing the most likely region to be deleted.

triose and other short oligosaccharides (*15*), it is likely that the glucosyl unit is missing because of enzymatic action rather than crystallographic disorder. The aromatic iodobenzyl group in site A stacks on the ionized, planar guanido group of Arg^{251}. Although arginine residues stacking on aromatic groups are found in active sites and sugar-binding sites (*16*), stacking of a guanido group onto a glucosyl unit is unusual. Normally, stacking interactions position the arginine side chain to form hydrogen bonds with the hydroxyls of the sugar. Site B resembles a typical sugar-binding site with the more hydrophobic β face of the glucosyl unit stacking on the indole ring of Trp^{376}. All hydroxyl groups of the sugar form hydrogen bonds to protein atoms or water molecules. The vacant C site contains Trp^{367} which, in a modeled, extended cellobioside, would interact with the α-face of the second sugar. A similar situation exists in the active site of CBHII where indole rings interact with both α and β faces of glucosyl units (*10*). Two more tryptophan residues (38 and 40) line the other end of the tunnel to form site E and the last site, G.

Cellobiohydrolase I, like lysozyme, cleaves β-1,4-glycosidic bonds with retention of configuration, yielding the β anomer as reaction product (*7*). The necessary catalytic residues for a double-displacement reaction (*17*) are immediately apparent from the CBHI structure. The third strand of the concave sheet contains three acidic residues (Glu^{212}, Asp^{214}, and Glu^{217}) that are close to the proposed β(1 → 4) linkage between sites B and C. Because of the curvature of the strand, the carboxylate groups wrap around the acetal linkage such that Glu^{217} is "below" and Glu^{212} "above" the bond to be cleaved (Fig. 1). The strand curvature is increased by an irregularity so that the side chains of residues Ile^{215} and Trp^{216} are both internal. Both Glu^{217} and Asp^{214} form hydrogen bonds to hydroxyl groups of the glucosyl unit in site B. The Glu^{217} hydrogen bonds to O-4 [equivalent to the β(1 → 4)–linking oxygen in the cellobioside] and to O-3, whereas Asp^{214} interacts only with the O-3 hydroxyl. The carboxylate of Asp^{214} is also in close contact with the carboxylate of Glu^{212} (214 OD1–212 OE2 2.7 Å) and to the imadazole ring of His^{228} from a neighboring strand (214 OD2–228 NE2 3.1 Å). In turn, Glu^{212} makes contacts to Ser^{174} (212 OE1–174 OG 2.8 Å and 212 OE1–174 N 3.1 Å) and has three hydrogen bonds to water molecules. Although all three residues are likely to be important, the proximity of Glu^{217} to the O-4 atom suggests that this residue may act as a general acid catalyst by donating a proton. The proximity of the side chains of Glu^{212}, Asp^{214}, and His^{228} are likely to affect their p*K*'s but, based on its position and environment, we think that Glu^{212} is the probable nucleophile. The active site residues are highly conserved when the nine available sequences of CBHIs and the related EGI endoglucanases are aligned (*18*). Our proposal that cleavage occurs between sites B and C is in agreement with the binding studies and suggests that the cellulose chain is cleaved from its reducing end (*19*). It also explains why the preferred product is cellobiose and not glucose for longer substrates because the restricted volume prevents extensive rearrangement of the cellulose chain as it threads through the tunnel. The zig-zag pattern of glycosidic linkages then allows the correct conformation to occur at the active site every two glucosyl units, giving rise to the cellobiose product.

On the basis of the CBHII structure, it was proposed that several loops making up the active site of exoglucanases have been lost during the evolution of related endoglucanses to create more open structures (*10*). This has been confirmed in the CBHII family by the structure determination of the related endoglucanase E230 (*11*). A comparison of the sequences of CBHI and the homologous endoglucanase EGI from *T. reesei* (*20*) revealed several deletions in the endoglucanase sequence. Four of these deletions map to active site loops in CBHI that help to form the substrate binding tunnel (Fig. 3), supporting the hypothesis that endoglucanases are generated from related exoglucanases by active site loop deletion.

The active site of CBHI shows local similarities to a number of carbohydrate-degrading enzymes, each of very different structure (*21*). The CBHI core also shows unexpected overall structural similarity to two families of proteins; the legume lectins and a family of bacterial 1,3-1,4-β-glucanases (also called lichenases and β-glucanases). The similarity to the legume lectins is essentially at the level of the folding topology (*22*). Though the comparison of CBHI with lysozymes is an example of convergent evolution, a comparison with a *Bacillus* β-glucanase structure (*23*) reveals evidence for a direct evolutionary relation. The structures can be superimposed such that 131 pairs of Cα atoms (out of the 214 residues in the β-glucanase) have a root-mean-square (rms) deviation of 1.8 Å. These residues correspond to most of the β sandwich in the β-glucanase. The long loops that form the tunnel in CBHI are missing in the β-glucanase which cleaves β(1 → 4) bonds in the middle of mixed linked β-glucan chains that also contain β(1 → 3) linkages. Their requirement for an open active site is, therefore, in agreement with the exo-endo hypothesis described above. Only 12 residues are conserved in sequence within the structural alignment, but they include the catalytic trio of carboxylates and both tryptophans in the active site. The residue structurally equivalent to the suggested nucleophile in CBHI (Glu^{212}) has been identified as the likely catalytic nucleophile in the β-glucanase (*24*).

We believe that the key to understanding the primary function of CBHI is the long cellulose binding tunnel. The relative-

ly low catalytic efficiency of the enzyme (*15*) has already raised the question of whether hydrolysis is its primary function and whether the genes encoding cellobiohydrolases are under any selection pressure to increase their catalytic efficiency (*25*). The differing tunnels observed in CBHI and CBHII can explain both their synergy and their interaction with crystalline cellulose. The sorption of CBHI is rapid and irreversible. The distribution of the enzymes on cellulose crystals is markedly different; CBHI shows a preference for the crystal edge (*26*), but CBHII acts at one tip of the crystal (*27*). In CBHII, the active site tunnel is relatively short so that after cellobiose has been produced, the remaining cellulose chain may either fall off the enzyme or thread further into the tunnel, thereby leading to another cycle of activity. Therefore, the clustering of CBHII at one tip is due to the continuous attachment and separation of the enzyme to the free nonreducing ends of cellulose chains. If a cellulose chain threads into the CBHI tunnel from the A site, we would also expect the cellulose to eventually fall off the enzyme. However, if the entry is from the G site, the length of the CBHI tunnel makes it more likely that the cellulose chain remains attached to the enzyme after the catalytic reaction, and the enzyme then progresses along the chain. This results in the enzyme coating the cellulose surface with a preference for the more exposed crystal edge. The synergistic action of CBHI and CBHII is most simply explained if we assume that one or both of the enzymes has some endoglucanase activity (*28*). However, as CBHI pares the crystal by peeling off one cellulose chain at a time, the interactions between neighboring chains may be weakened, making them easier to separate and more accessible to hydrolysis by CBHII.

REFERENCES AND NOTES

1. T. M. Wood, in *Enzyme Systems for Lignocellulose Degradation*, M. P. Coughlan, Ed. (Elsevier, London and New York, 1989), pp. 19–35.
2. Hypercellulolytic mutants of the filamentous fungus *T. reesei* produce more than 20 g of cellulolytic enzymes per liter of their culture medium [M. J. Bailey and K. M. H. Nevalainen, *Enzyme Microb. Technol.* **3**, 153 (1981); H. Durand, M. Clanet, G. Tiraby, *ibid.* **10**, 341 (1988)]. Cellobiohydrolase I is by far the most abundant single cellulase in this mixture, comprising ~60% of the total cellulolytic protein [M. Gritzali and R. D. Brown, *Adv. Chem. Ser.* **181**, 237 (1979); M. Nummi, M.-L. Niku-Paavola, A. Lappalainen, T.-M. Enari, V. Raunio, *Biochem. J.* **215**, 677 (1983)]. Cellobiohydrolase I is also the most abundant cellulase in other potent cellulose-degrading organisms such as *Penicillium pinophilum, Phanerochaete chrysosporium*, and others (*1*). The selective removal of the CBHI gene has the greatest effect on overall activity on crystalline cellulose [P. L. Suominen, A. L. Mänyla, T. Karhunen, S. Hakola, H. Nevalainen, *Mol. Gen. Genet.* **241**, 253 (1993)].
3. B. Nidetzky *et al.*, *Biochem. J.* **298**, 705 (1994); D. C. Irwin *et al.*, *Biotechnol. Bioeng.* **42**, 1002 (1993). Whereas only a number of substrate sites are available on filter paper for hydrolysis by EGs, CBH sites are not depleted.
4. L. G. Fägerstam and L. G. Pettersson, *FEBS Lett.* **119**, 97 (1980).
5. B. Henrissat *et al.*, *Biotechnology* **3**, 722 (1985); M.-L. Niku-Paavola *et al.*, *Biotechnol. Appl. Biochem.* **8**, 449 (1986); J. Ståhlberg *et al.*, *Biochim. Biophys. Acta* **1157**, 107 (1993).
6. B. Henrissat, *Biochem. J.* **280**, 309 (1991); ——— and A. Bairoch, *ibid.* **293**, 781 (1993).
7. J. K. C. Knowles *et al.*, *J. Chem. Soc. Chem. Commun.* **1988**, 1401 (1988); M. Claeyssens *et al.*, *FEBS Lett.* **263**, 89 (1990).
8. P. Tomme *et al.*, *Eur. J. Biochem.* **170**, 575 (1988); P. M. Abuja *et al.*, *Eur. Biophys. J.* **15**, 339 (1988).
9. Cellobiohydrolase I is able to act as a chiral selector for the separation of the enantiomers of a number of small molecules such as the β-adrenergic blocker propranolol [I. Marle, S. Jönsson, R. Isaksson, C. Pettersson, G. Pettersson, *J. Chromatogr.* **648**, 333 (1993)]. Because of the restricted space and the possibility of making many specific interactions, the tunnel is likely to be the binding site for these molecules, and a number of β blockers have been found to inhibit the enzyme [J. Ståhlberg, S. Jönsson, G. Pettersson, in Trichoderma reesei *Cellulases and Other Hydrolases*, P. Suominen and T. Reinikainen, Eds. (Foundation for Biotechnical and Industrial Fermentation Research, Finland, 1993), pp. 273–280].
10. J. Rouvinen *et al.*, *Science* **249**, 380 (1990).
11. M. Spezio, D. B. Wilson, P. A. Karplus, *Biochemistry* **32**, 9906 (1993).
12. M. Juy *et al.*, *Nature* **357**, 89 (1992).
13. G. J. Davies *et al.*, *ibid.* **365**, 362 (1993).
14. N. K. Vyas, *Curr. Opin. Struct. Biol.* 1, 732 (1986). We use the same definition for the α and β faces of glucosyl units.
15. Early studies suggested that the active site spanned only three glucosyl units [M. Claeyssens, H. van Tilbeurgh, P. Tomme, T. M. Wood, S. I. McCrae, *Biochem. J.* **261**, 819 (1989)]. This has expanded to a site containing at least six glucosyl units [B. Nidettzky, W. Zachariae, G. Gercken, M. Hayn, W. Steiner, *Enzyme Microb. Technol.* **16**, 43 (1994)].
16. M. M. Flocco and S. L. Mowbray, *J. Mol. Biol.* **235**, 709 (1994).
17. D. E. Koshland Jr., *Biol. Rev.* **28**, 416 (1953).
18. In our alignments (*30*), Glu^{217} is fully conserved, and the residues at both 212 and 214 are conserved in all but one sequence where 212 is an aspartic acid and 214 is an alanine residue. In addition, His^{228} and Trp^{376} are fully conserved, whereas the other three tryptophans in the tunnel show some variation in either one or two of the sequences. Our position of the active site differs from one report in the literature. It has been suggested on the basis of chemical modification studies that Glu^{126} is essential for catalysis [P. Tomme and M. Claeyssens, *FEBS Lett.* **243**, 239 (1989)]. Site-directed mutagenesis of Glu^{126} to an alanine gave an enzyme that retained 29% of the wild-type activity [Y. Mitsuishi *et al.*, *ibid.* **275**, 135 (1990)]. This in turn suggested that the residue was not directly involved in catalysis but may be located in the active site and involved in substrate binding. It is, in fact, positioned on the convex face of the β sandwich, pointing out into the solvent, ~20 Å from the cellulose-binding tunnel.
19. Because both ends of the tunnel are open to the solvent, the cellulose chain could in principle enter from either end. If the entire length of the tunnel is used to interact with the substrate, site G would be at the entrance and A at the exit. The observed orientation of the ligand in the tunnel then suggests that the enzyme cleaves the cellulose chain from its reducing end. This is in agreement with data obtained with small oligosaccharides as substrates [M. Vrsanská and P. Biely, *Carbohydr. Res.* **227**, 19 (1992)]. Substrate entry from site A would lead to hydrolysis from the nonreducing end, and the cellobiose product would then need to diffuse along the entire length of the tunnel.
20. M. Penttilä *et al.*, *Gene* **45**, 253 (1986).
21. Hen egg-white lysozyme (HEWL) [C. C. F. Blake *et al.*, *Nature* **206**, 757 (1965)], T4 lysozyme [W. F. Anderson, M. G. Grütter, S. J. Remington, L. H. Weaver, B. W. Matthews, *J. Mol. Biol.* **147**, 523 (1981)], and endoglucanase EGV (*13*) have extended binding sites that are formed by a cleft between two lobes with the catalytic residues positioned on either side. The catalytic residues of HEWL, Glu^{35}, and Asp^{52} can be superimposed onto the proposed functionally equivalent glutamic acids 217 and 212 of CBHI. Both are retaining enzymes, requiring a double-displacement mechanism. Interestingly, the catalytic residues in the inverting enzyme EGV are spatially arranged more as in HEWL than in CBHII which also acts with inversion.
22. Members of the legume lectin family are built from two or four identical subunits of ~25 kD. Each subunit has a carbohydrate-binding site that requires a bound calcium and manganese ion. They consist of a large β sandwich with the same strand topology as CBHI. We have not identified any sequence homology between the two families. Although concanavalin A (Con A) [G. M. Edelman *et al.*, *Proc. Natl. Acad. Sci. U.S.A.* **69**, 2580 (1972)] is only half the size of the CBHI core protein, their β sandwiches have roughly the same size and 45 pairs of Cα atoms of the central β strands can be superimposed with an rms deviation of 1.9 Å. The loops from the β sandwich are considerably shorter in the lectins than the corresponding loops in CBHI, and consequently no tunnel is formed. The metal ion binding sites are approximately positioned in the active site of CBHI (Glu^{8} in Con A coordinates a manganese ion and is structurally equivalent to residue Glu^{217} in CBHI). The sugar-binding site in the legume lectins is positioned in a depression on the protein surface adjacent to the calcium-binding site.
23. T. Keitel, O. Simon, R. Borriss, U. Heinemann, *Proc. Natl. Acad. Sci. U.S.A.* **90**, 5287 (1993).
24. In the β-glucanase family the structurally equivalent residue is Glu^{105}. Its role as the likely catalytic nucleophile has been determined by site-directed mutagenesis (*23*), by mechanism-based affinity labeling [P. B. Høj, R. Condron, J. C. Traeger, J. C. McAuliffe, B. A. Stone, *J. Biol. Chem.* **267**, 25059 (1992)], and by the structural work (*23*). There is one interesting difference in the active site strand. The sequence of this strand is $E^{212}MD^{214}IWE^{217}$ in CBHI but $E^{105}ID^{107}IE^{109}$ in the β-glucanase. In CBHI, both $I^{215}W^{216}$ are internal, forming part of the β sandwich core. Ile^{215} is an insert in CBHI that distorts the regular strand, producing the increased curvature that allows the trio of carboxylates to wrap around the substrate. Abbreviations for the amino acids are as follows: D, Asp; E, Glu; I, Ile; M, Met; and W, Trp.
25. A. K. Konstantinidis, I. Marsden, M. L. Sinnott, *Biochem. J.* **291**, 883 (1993).
26. H. Chanzy, B. Henrissat, R. Vuong, M. Schülein, *FEBS Lett.* **153**, 113 (1983).
27. H. Chanzy and B. Henrissat, *ibid.* **184**, 285 (1985).
28. One loop in each active site shows somewhat elevated temperature factors that may indicate areas that could open up the site to allow endoactivity. We judge that this is insufficient to open up the active site to a cellulose chain.
29. Crystals with typical dimensions of 0.3 mm by 0.3 mm by 0.2 mm were obtained as described [C. Divne *et al.*, *J. Mol. Biol.* **234**, 905 (1993)] but with the addition of *o*-iodobenzyl-1-thio-β-D-cellobioside to a final concentration of 1 mM. The complex crystals were isomorphous to the unliganded form with two molecules in the asymmetric unit and a solvent content of ~40%. The independent molecules are related by a fractional translation operator of (0.454, 0.500, 0.500) which prevented us from defining the space group until we had solved a heavy atom difference Patterson. Diffraction data were measured with both a Nicolet/Xentronics multiwire area detector and an R-AXIS IIC imaging plate system mounted on Rigaku rotating anode generators at +4°C. One of the heavy atom derivatives was made with crystals from a mutant enzyme where a free cysteine residue was introduced at Ser^{128} with site-directed mutagenesis. Heavy atom parameters were refined with the

program MLPHARE [Z. Otwinowski, in *Isomorphous Replacement and Anomalous Scattering*, W. Wolf, P. R. Evans, A. G. W. Leslie, Eds. (SERC Daresbury Laboratory, Warrington, Cheshire, U.K., 1991), pp. 80–85] in the CCP4 software package. Phases were improved by density modification [K. Y. J. Zhang and P. Main, *Acta Crystallogr.* **A46**, 377 (1990)] and twofold averaging [T. A. Jones, in *Molecular Replacement*, E. J. Dodson, Ed. (SERC Daresbury Laboratory, Warrington, Cheshire, U.K., 1992), pp. 91–105] at 3.5 Å resolution and then extended to 3 Å. The extension was made in steps of 0.1 Å and consisted of averaging, phase combination with the MIR phases, and density modification. The main chain was traced with O with skeletonized electron density, and the initial model built from a database of refined structures [T. A. Jones and S. Thirup, *EMBO J.* **5**, 819 (1986); T. A. Jones, J.-Y. Zou, S. W. Cowan, M. Kjeldgaard, *Acta Crystallogr.* **A47**, 110 (1991)]. The initial complete model had an *R* factor of 49.9% for reflections in the resolution range of 7.5 to 2.0 Å. Two rounds of simulated annealing [A. T. Brünger, J. Kuriyan, M. Karplus, *Science* **235**, 458 (1987)] and rebuilding reduced the *R* factor to 25.0%. Six cycles of standard least squares refinement and rebuilding gave a final *R* factor of 18.1% for all measured unique reflections in the resolution range 7.5 to 1.8 Å. This model contained 7038 nonhydrogen atoms corresponding to the complete amino acid sequence of both molecules, two *N*-acetyl glucoseamine molecules (one *N*-glycosylation site per molecule at Asn^{270}), two *o*-iodobenzyl-1-thio-β-D-glucose molecules, 529 water molecules, and one calcium atom (in a special position on the twofold axis). The model was tightly restrained with rms deviations in bond lengths, bond angles, fixed dihedral angles of 0.008 Å, 1.7°, and 1.4°, respectively. One nonglycine residue (Ser^{99}) has deviant main chain torsion angles, and 12 residues have "pep-flip" values greater than 2.5 Å. The two molecules in the asymmetric unit have an rms fit of 0.2 Å for all atoms. The surface in Fig. 3 was generated with Voidoo [G. J. Kleywegt and T. A. Jones, *Acta Crystallogr.* **D50**, 178 (1994)].

30. C. Divne *et al.*, data not shown.
31. We thank U. Heinemann for Cα coordinates of the β-glucanase before their general release and P. Laamanen and T. Kuurila for skillful technical assistance. This work has been supported by the Swedish Natural Science Research Council, Nordisk Industrifond, and Alko Limited. The coordinates have been deposited at the Protein Data Bank at Brookhaven.

8 February 1994; accepted 17 May 1994

Fas and Perforin Pathways as Major Mechanisms of T Cell–Mediated Cytotoxicity

David Kägi,* Françoise Vignaux,* Birgit Ledermann, Kurt Bürki, Valérie Depraetere, Shigekazu Nagata, Hans Hengartner, Pierre Golstein†

Two molecular mechanisms of T cell–mediated cytotoxicity, one perforin-based, the other Fas-based, have been demonstrated. To determine the extent of their contribution to T cell–mediated cytotoxicity, a range of effector cells from normal control or perforin-deficient mice were tested against a panel of target cells with various levels of Fas expression. All cytotoxicity observed was due to either of these mechanisms, and no third mechanism was detected. Thus, the perforin- and Fas-based mechanisms may account for all T cell–mediated cytotoxicity in short-term in vitro assays.

T cell–mediated cytotoxicity has been studied over many years (*1*). Two mechanisms have been defined at the molecular level. A perforin-based mechanism (*2*) was confirmed by the low cytotoxic activity of activated lymphoid cell populations from perforin-deficient (P°) mice obtained by gene targeting (*3*). This mechanism seems to require molecules other than perforin, including certain serine esterases (*4*). Independently, a Fas-based mechanism was molecularly defined through involvement at the target cell level (*5*) of the cell death–transducing molecule Fas (APO-1) (*6*) and at the effector cell level of a Fas ligand (*7*). We investigated whether these two mechanisms could account for all T cell–mediated cytotoxicity.

We first examined the specific antialloge-neic cytotoxicity generated in mixed leukocyte cultures (MLCs) in vitro (*8*). Wild-type C57BL/6–anti-C3H (H-2b–anti–H-2k; b–anti-k) MLC cells lysed thymocytes from wild-type C3H (k) mice in a 4-hour ^{51}Cr release assay (*9*) (Fig. 1A). They also lysed thymocytes from *lpr* mutant k mice (*10*), which express little or no Fas (*11*) and are thus unable to be lysed by the Fas-based mechanism (Fig. 1B). When P° b–anti-k MLC cells, which are unable to lyse through the perforin-based pathway, were used as effector cells, some cytotoxicity still occurred on wild-type thymocytes (Fig. 1C), but not on *lpr* thymocytes (Fig. 1D). The simplest interpretation for this absence of cytotoxicity is that when effectors were unable to exert perforin-based lysis and targets were unable to be lysed through the Fas pathway, no other mechanism operated. In confirmation of other results (*3*, *5*), both perforin- and Fas-based mechanisms were antigen-specific because in all cases k, but not C57BL/6 (b), thymocytes were lysed (Fig. 1, A through C).

Similar evidence was obtained with nonantigen-specific stimuli. MLC cells from wild-type mice could be induced by phorbol 12-myristate 13-acetate (PMA) plus ionomycin to lyse syngeneic target cells through the Fas-based mechanism and by concanavalin A (Con A) to lyse the same syngeneic target cells by a mechanism that was not Fas-based (*12*). C57BL/6–anti-BALB/c (b–anti-d) MLC cells, either wild-type or P°, were tested against syngeneic b thymocytes, either wild-type or *lpr*. In medium alone, no cytotoxicity was detected in this syngeneic combination (Fig. 1, E through H). In the presence of PMA plus ionomycin, wild-type MLC cells lysed wild-type thymocytes (Fig. 1E), but not *lpr* thymocytes (Fig. 1F), confirming that in this system PMA plus ionomycin reveals the Fas-based pathway exclusively (*12*). The same results were obtained with P° MLC cells (Fig. 1, G and H), leading to the conclusion that P° cells could be induced by PMA plus ionomycin to exert Fas-based cytotoxicity against syngeneic cells.

Lysis of both wild-type and *lpr* thymocytes by wild-type MLC cells stimulated by Con A (Fig. 1, E and F) confirmed that Con A triggered a non–Fas-based mechanism of cytotoxicity. Con A also triggered lysis by P° MLC cells of wild-type thymocytes (Fig. 1G) but not of *lpr* thymocytes (Fig. 1H). The simplest interpretation of these findings is that Con A induces both perforin- and Fas-based mechanisms. Neither can operate when P° effectors, which are unable to exert perforin-based cytotoxicity, are used with *lpr* target cells (Fig. 1H). Thus, in this experimental system (Fig. 1, E through H), although Con A could trigger both perforin- and Fas-based cytotoxicity, no other cytotoxicity mechanisms were revealed.

These conclusions also held for experiments that used target cells other than thymocytes. Wild-type or P° b–anti-d MLC cells were tested on L1210 or L1210-Fas tumor target cells, which express (*5*) little or more significant amounts of Fas, respectively. Whereas both target cells were lysed to about the same extent by wild-type mouse MLC cells (Fig. 2A), L1210 cells were lysed less efficiently than L1210-Fas cells by P° MLC cells (Fig. 2B) and by d11S cells, which can be considered prototypic Fas-based killer cells (Fig. 2C) (*5*, *13*). Cytotox-

D. Kägi and H. Hengartner, Institute of Experimental Immunology, Department of Pathology, University of Zürich, CH-8091 Zürich, Switzerland.
F. Vignaux, V. Depraetere, P. Golstein, Centre d'Immunologie INSERM-CNRS de Marseille-Luminy (CIML), Case 906, 13288 Marseille Cedex 9, France.
B. Ledermann and K. Bürki, Preclinical Research, Sandoz Pharma, CH-4002 Basel, Switzerland.
S. Nagata, Osaka Bioscience Institute, 6-2-4 Furuedai, Suita, Osaka 565, Japan.

*These authors contributed equally to this work.
†To whom correspondence should be addressed.